



Published in final edited form as:

*Biomacromolecules*. 2006 February ; 7(2): 483–490. doi:10.1021/bm050672n.

## Effects of Polymer Structure on the Inhibition of Cholera Toxin by Linear Polypeptide-Based Glycopolymers

Brian D. Polizzotti and Kristi L. Kiick \*

Department of Materials Science and Engineering and Delaware Biotechnology Institute, University of Delaware, 201 DuPont Hall, Newark, Delaware 19716

### Abstract

A variety of important biological events are mediated by the multivalent interaction between relevant oligosaccharides and multiple saccharide receptors on lectins, toxins, and cell surfaces; a variety of glycopolymeric materials have therefore been investigated in studies aimed at manipulating these events. The synthesis of protein and polypeptide-based glycopolymers via protein engineering and other methods offers opportunities to control both the number and the spacing of saccharides on a scaffold, as well as the conformation of the polymer backbone, and will therefore facilitate the structure-based design of polymers for inhibition of multivalent binding events. In initial studies, we have synthesized a family of galactose-functionalized glycopolymers with a poly(L-glutamic acid) backbone, in which the density and linker length of the pendant carbohydrate moiety were varied. The composition of the glycopolymers was determined via  $^1\text{H}$  NMR spectroscopy, and the impact of saccharide density and linker length, as well as the potential for these polypeptide-based glycopolymers to act as high-affinity inhibitors of the cholera toxin, has been indicated via competitive enzyme-linked immunosorbent assay and fluorescence titration experiments. The results of these studies suggest strategies for optimizing the binding of linear glycopolymers to bacterial toxins and will aid in the design of additional protein-based materials for studying the impact of multivalency, spacing, and backbone rigidity in a variety of biologically relevant binding events.

### Introduction

Protein-carbohydrate interactions mediate a variety of critical biological recognition processes such as those involved in cell signaling, organogenesis, fertilization, and inflammation, as well as the adhesion of various viral and bacterial toxins.<sup>1–4</sup> Therapies aimed at disrupting carbohydrate-mediated adhesion can target the oligosaccharide-toxin recognition event, but the low intrinsic affinity of carbohydrate-protein interactions hampers the development of low-molecular-weight inhibitors. Nature circumvents this weak affinity by displaying multiple copies of both the carbohydrate ligands and their protein receptors on the surfaces of interacting moieties; enhanced activities result from the resulting cluster glycoside effect.<sup>5</sup> Various factors that are known to influence the affinity and specificity of multivalent binding events include the structure of the individual saccharide residues, the structural features of the template upon which the saccharide residues are displayed, and the relative spatial orientation of the saccharide recognition elements.<sup>5</sup>

There has been a great deal of attention directed toward the development of polymer-derived multivalent ligands as both inhibitors and effectors of various biological processes.<sup>6–11</sup> For example, polymers decorated with varying degrees of sulfated galactose residues have been shown to induce shedding of cell surface L-selectin from neutrophils,<sup>12</sup> while a tailored

\*Corresponding author: email kiick@udel.edu.

template synthesis approach has been applied to design glycopolymers that bind the mannose-binding proteins concanavalin A (ConA) and lens culinaris agglutinin (LCA).<sup>13</sup> Glycopolymers decorated with sialyloligosaccharides have been produced for the inhibition of infection by the influenza viruses,<sup>14,15</sup> and dendrimeric materials have also been functionalized with a variety of saccharides to mediate multivalent binding events.<sup>6,9,16,17</sup> The impact of architecture on the inhibitory or effector activity of a variety of synthetic and protein-derived glycopolymers has been shown in multiple investigations, further demonstrating that variations in macromolecular structure can have a marked impact on the activities displayed by a specific glycopolymer.<sup>11,16,18</sup> Accordingly, of particular interest in our investigations is the development of protein-based glycopolymeric materials that can be used to study and manipulate interactions between saccharides and their receptors. The use of polypeptides facilitates studies aimed at the effect of backbone conformation (e.g., random coil versus helical) on the binding event; in addition, it may also be possible to enhance the binding event through protein–protein as well as saccharide–protein interactions. Furthermore, the design of artificial protein polymers will afford additional opportunities to precisely specify the number and placement of saccharides on the polymer chain. Such polypeptide and protein-based glycopolymers could be used to modulate multiple types of protein–carbohydrate interactions.

One active area of research in which such polymeric materials could be useful includes the development of antagonists aimed at disrupting the adhesion of bacterial toxins to cellular surfaces. For example, several groups have taken advantage of the receptor-binding process as a target for the structure-based design of multivalent antagonists against infection by various AB<sub>5</sub> toxins, including the cholera toxin (CT), shiga-like toxins (SLT-I and SLT-II), and the heat-labile enterotoxin (LT).<sup>19–30</sup> The AB<sub>5</sub> bacterial toxins consist of an enzymatically active A subunit and five identical B subunits that organize into a regular pentamer and mediate adhesion to the host cell. Infection by CT is initiated when the B<sub>5</sub> subunit, with five identical saccharide-binding sites, interacts with the receptor ganglioside GM1 (Galβ1-3GalNAcβ1-4 (Neu5Acα2-3)Gal-β1-4Glc-ceramide) that is present on the surface of human intestinal epithelial cells. Once the toxin is bound, it becomes internalized via receptor-mediated endocytosis, upon which the toxic A subunit is cleaved and initiates a series of events that results in host dehydration and diarrhea.<sup>31</sup>

A variety of small-molecule pentameric inhibitors with submicromolar AB<sub>5</sub> toxin binding have resulted from these investigations,<sup>21,30,32</sup> and linear scaffolds with low micromolar inhibitory activity for CT and SLT have also been reported. Specifically, a series of short linear bivalent ligands have been produced as inhibitors of the CT B<sub>5</sub> subunit,<sup>33</sup> whereas monoand difunctionalized C-linked glycopeptides have been investigated as ligands for SLT-1B.<sup>34</sup> Although these linear molecules have not demonstrated as efficient inhibition of CT as the pentameric small-molecule structures, the successful application of a linear architecture may offer opportunities for producing a broader range of inhibitors for a greater number of targets than a small molecule approach.

In this work, we have produced linear multivalent inhibitors based on a poly(L-glutamic acid) (PGA) backbone, in which the density and linker length of the pendant carbohydrate moiety were varied. The cholera toxin was chosen for inhibition in these studies because of its ability to bind to multivalent displays of simple monosaccharides, coupled with the lack of reported linear macromolecular antagonists for the inhibition of AB<sub>5</sub> toxins. There has been little use of polypeptidic-based backbones as scaffolds for the inhibition of CT B<sub>5</sub>,<sup>30</sup> although glycosylated poly(L-glutamic acid) has been shown to inhibit the binding of various plant lectins<sup>35–37</sup> and has been used as a scaffold in the synthesis of multivalent inhibitors of the influenza virus.<sup>15,38</sup> The carboxylic acid functionality of PGA allows the coupling of various types of amine-functionalized saccharides, which provides a facile way to explore the role of

density and length of the linker arm in the binding of linear glycopolymers to CT. Accordingly, a series of PGA-based glycopolymers were synthesized, with varying saccharide density and linker arm length. The potential for these random-coil polypeptide-based glycopolymers as high-affinity inhibitors of the cholera toxin has been indicated via both competitive enzyme-linked immunosorbent assay and fluorescence titration experiments. The results from these studies will act as a guide in the design of other linear artificial protein-based glycopolymers, in which both the spacing and the number of saccharides on a polymer chain can be controlled.

## Experimental Section

### Materials and Methods

2-(1H-Benzotriazole-1-yl)-1,1,3,3-tetra-methyluronium hexafluorophosphate (HBTU) and Fmoc-6-aminohexanoic acid (Fmoc-Ahx-OH) were obtained from EMD Biosciences Inc. (San Diego, CA). The cholera toxin B<sub>5</sub> subunit (CT B<sub>5</sub>) and cholera toxin B<sub>5</sub> subunit horseradish peroxidase conjugate (CT B<sub>5</sub>-HRP) were obtained from List Biological Laboratories (Campbell, CA). Ganglioside GD1b was obtained from Matreya (Pleasant Gap, PA). C96 Maxisorp microtiter plates were obtained from Fisher Scientific (Pittsburgh, PA). The deionized water was generated from a Barnstead Diamond water purification system (Barnstead, Dubuque, IA, 18.1 MΩ-cm resistivity). Poly(L-glutamic acid) (PGA, DP = 113, MW = 15 000–50 000), β-D-galactosylamine, N-(ε-aminocaproyl)-β-D-galactosylamine, dimethyl sulfoxide (DMSO), diisopropylethylamine (DIPEA), and all other reagents were obtained from Sigma-Aldrich Co. (St. Louis, MO) and used as received without any further purification. <sup>1</sup>H NMR spectra were acquired on a Bruker DRX-400 NMR spectrometer. The samples were prepared by dissolving 5 mg of sample into 350 μL of dimethyl sulfoxide-*d*<sub>6</sub> (DMSO-*d*<sub>6</sub>) or deuterium oxide. The resulting solutions were placed in 5 mm NMR tubes, and the spectra were recorded under standard quantitative conditions at ambient temperature.

### Preparation of PGA

The PGA was precipitated according to the method of Zeng.<sup>35</sup> Briefly, 1 g of the poly(L-glutamic acid) sodium salt was dissolved in 20 mL of ice-cold water, and 5.2 mL of 1 N hydrochloric acid solution was added dropwise to the solution with stirring for 2 h. The precipitate was collected via centrifugation (4 °C, 4000 × g, 5 min) and washed three times with cold water. Finally, the suspension was lyophilized, affording protonated PGA in approximately 65% yield. <sup>1</sup>H NMR of PGA (DMSO, 25 °C, 400 MHz): δ 3.96 (113H, peptide α-methine NHCHCO), δ 2.27 (226H, peptide γ-methylene CHCH<sub>2</sub>CH<sub>2</sub>), δ 1.93 (226H, peptide β-methylene CHCH<sub>2</sub>CH<sub>2</sub>).

### Synthesis of N-(ε-aminocaproyl)-β-D-galactosylamine

Fmoc-Ahx-OH (100 mg, 280 μmol) was dissolved in DMSO (500 μL). Then, DIEA (243 μL, 1.4 mmol) and HBTU (106 mg, 280 μmol) were added to the solution, and the mixture was allowed to preactivate for approximately 5 min. In a separate vial, β-D-galactosylamine (50 mg, 280 μmol) was dissolved in DMSO (1 mL). The solution was heated slightly to completely dissolve the saccharide. After the solution cooled to room temperature, the saccharide solution was added to the activated solution. The mixture was allowed to react at room temperature with constant stirring for 5 h. The final mixture was diluted with methylene chloride (DCM, 10 mL), and the desired product was extracted via treatment with water (3×, 25 mL). Analysis of the extracted product via HPLC and electrospray-ionization MS indicated the presence of the desired product and the absence of any starting materials. The aqueous phase was then freeze-dried to yield the Fmoc-protected saccharide. Deprotection of the Fmoc group was carried out by treatment with 20% piperidine in DMF (10 mL) for 2 h at room temperature with constant stirring. The deprotected saccharide was then precipitated via addition of cold ethyl ether and collected via centrifugation (4000 × g, 4 °C, 5 min). The precipitate was then

washed with ethyl ether (3×, 25 mL) and again freeze-dried to yield the title compound in 80% yield. <sup>1</sup>H NMR (D<sub>2</sub>O, 25 °C, 400 MHz): δ 4.81 (1H, anomeric proton), δ 3.87 (1H, Gal H-2 proton), δ 3.49–3.68 (5H, Gal ring protons from Gal unit), δ 2.75 (2H, methylene group N<sub>2</sub>HCOCH<sub>2</sub>CH<sub>2</sub>CH<sub>2</sub>CH<sub>2</sub>CH<sub>2</sub>NH<sub>2</sub>), δ 2.32 (2H, methylene group N<sub>2</sub>HCOCH<sub>2</sub>CH<sub>2</sub>CH<sub>2</sub>CH<sub>2</sub>CH<sub>2</sub>NH<sub>2</sub>), δ 1.25–1.65 (6H, methylene groups N<sub>2</sub>HCOCH<sub>2</sub>CH<sub>2</sub>CH<sub>2</sub>CH<sub>2</sub>CH<sub>2</sub>NH<sub>2</sub>).

### General Procedure for the Preparation of Glycopolymers 1–6

The compounds of varying saccharide density were synthesized by varying the molar ratio of the desired amino-functionalized saccharide with respect to the number of carboxylic acid residues along the PGA backbone. The estimated number of moles of carboxylic acid residues in a given sample of PGA was based on the manufacturer's reported degree of polymerization of 113. The general synthetic procedure was as follows (with details specific for compound **5**; β-D-galactosylamine was used for compounds **1–3** and *N*-(ε-Aminocaproyl)-β-D-galactosylamine for compounds **4–6**): *N*-(ε-Aminocaproyl)-β-D-galactosylamine (7.8 mg, 26.7 μmol) was dissolved in 1 mL of DMSO. The solution was heated slightly to help dissolve the saccharide. The solution was cooled to room temperature, and precipitated PGA (20 mg, 26.7 μmole COOH) was added. The solution was stirred at room temperature until the PGA was completely dissolved. Then, DIEA (46.5 μL, 267 μmol) and HBTU (10.12 mg, 26.7 μmol) were added, and the reaction was stirred at room temperature overnight. The solution was then diluted with water and placed into dialysis tubing (1000 MWCO) and dialyzed against 1 M NaCl (48 h, four changes, 1 L each time) to remove impurities from the coupling reaction, followed by dialysis against MilliQ water (48 h, four water changes, 1 L each time) to remove the sodium chloride. The solution was then lyophilized to yield **5** as a white solid. Glycopolymers **1–6** were all synthesized in duplicate. <sup>1</sup>H NMR data for compounds **1–6** are given below.

<sup>1</sup>H NMR data of **1** (D<sub>2</sub>O, 25 °C, 400 MHz): δ 4.38 (113H, polypeptide α-methine NHCHCO), δ 4.02 (13H, Gal H-2 proton), δ 3.60–3.90 (65H, ring protons from Gal unit), δ 2.38 (226H, polypeptide γ-methylene CHCH<sub>2</sub>CH<sub>2</sub>), δ 2.06 (226H, polypeptide β-methylene CHCH<sub>2</sub>CH<sub>2</sub>).

<sup>1</sup>H NMR data of **2** (D<sub>2</sub>O, 25 °C, 400 MHz): δ 4.31 (113H, polypeptide α-methine NHCHCO), δ 3.96 (23H, Gal H-2 proton), δ 3.60–3.88 (115H, ring protons from Gal unit), δ 2.37 (226H, polypeptide γ-methylene CHCH<sub>2</sub>CH<sub>2</sub>), δ 2.07 (226H, polypeptide β-methylene CHCH<sub>2</sub>CH<sub>2</sub>).

<sup>1</sup>H NMR data of **3** (D<sub>2</sub>O, 25 °C, 400 MHz): δ 4.32 (113H, polypeptide α-methine NHCHCO), δ 3.97 (56H, Gal H-2 proton), δ 3.51–3.91 (280H, ring protons from Gal unit), δ 2.39 (226H, polypeptide γ-methylene CHCH<sub>2</sub>CH<sub>2</sub>), δ 2.07 (226H, polypeptide β-methylene CHCH<sub>2</sub>CH<sub>2</sub>).

<sup>1</sup>H NMR data of **4** (D<sub>2</sub>O, 25 °C, 400 MHz): δ 4.29 (113H, polypeptide α-methine NHCHCO), δ 3.95 (11H, Gal H-2 proton), δ 3.59–3.90 (55H, ring protons from Gal unit), δ 3.14 (22H, methylene–N<sub>2</sub>HCOCH<sub>2</sub>CH<sub>2</sub>CH<sub>2</sub>CH<sub>2</sub>CH<sub>2</sub>NH<sub>2</sub>), δ 1.32–1.65 (88H, methylene groups –N<sub>2</sub>HCOCH<sub>2</sub>CH<sub>2</sub>CH<sub>2</sub>CH<sub>2</sub>CH<sub>2</sub>NH<sub>2</sub>), δ 2.36 (226H, polypeptide γ-methylene CHCH<sub>2</sub>CH<sub>2</sub>), δ 2.05 (226H, polypeptide β-methylene CHCH<sub>2</sub>CH<sub>2</sub>).

<sup>1</sup>H NMR data of **5** (D<sub>2</sub>O, 25 °C, 400 MHz): δ 4.35 (113H, polypeptide α-methine NHCHCO), 4.01 (25H, Gal H-2 proton), δ 3.61–3.92 (125H, ring protons from Gal unit), δ 3.18 (50H, methylene–N<sub>2</sub>HCOCH<sub>2</sub>CH<sub>2</sub>CH<sub>2</sub>CH<sub>2</sub>CH<sub>2</sub>NH<sub>2</sub>), δ 1.35–1.65 (200H, methylene groups –N<sub>2</sub>HCOCH<sub>2</sub>CH<sub>2</sub>CH<sub>2</sub>CH<sub>2</sub>CH<sub>2</sub>NH<sub>2</sub>), δ 2.36 (226H, polypeptide γ-methylene CHCH<sub>2</sub>CH<sub>2</sub>), δ 2.05 (226H, polypeptide β-methylene CHCH<sub>2</sub>CH<sub>2</sub>).

$^1\text{H}$  NMR data of **6** (DMSO, 25 °C, 400 MHz):  $\delta$  4.23 (113H, polypeptide  $\alpha$ -methine NHCHCO),  $\delta$  4.79 (113H, Gal H-2 proton),  $\delta$  3.68–4.70 (565H, ring protons from Gal unit),  $\delta$  3.01 (226H, methylene–NHCOCH<sub>2</sub>CH<sub>2</sub>CH<sub>2</sub>CH<sub>2</sub>CH<sub>2</sub>NH<sub>2</sub>),  $\delta$  1.23–1.48 (904H, methylene groups –NHCOCH<sub>2</sub>CH<sub>2</sub>CH<sub>2</sub>CH<sub>2</sub>CH<sub>2</sub>NH<sub>2</sub>),  $\delta$  2.09 (226H, polypeptide  $\beta$ -methylene CHCH<sub>2</sub>CH<sub>2</sub>),  $\delta$  1.88 (226H, polypeptide  $\beta$ -methylene CHCH<sub>2</sub>CH<sub>2</sub>).

### CT GD1b Direct Enzyme-Linked Assay

A direct-linked enzyme assay based on the assay reported by Minke et al.<sup>25</sup> was employed to assess the binding of the glycopolymers to CT. Microtiter plates were incubated at 37 °C for 16 h with 100  $\mu\text{L}$  of 2  $\mu\text{g}/\text{mL}$  ganglioside GD1b dissolved per well in phosphate-buffered saline (pH 7.2) containing 150 mM NaCl and 10 mM potassium phosphate (PBS). Unattached ganglioside was removed by washing the wells three times with PBS. Additional binding sites on the plate surface were blocked by incubating the wells with 200  $\mu\text{L}$  of a 1% (w/v) bovine serum albumin (BSA)–PBS solution for 30 min at 37 °C and then washing them three times with 0.05% Tween 20–PBS. Test samples (see below), diluted in 0.1% BSA–0.05% Tween 20–PBS, were added in 100  $\mu\text{L}$  volumes per well and incubated for 30 min at room temperature. Unbound toxin was removed by washing three times with 0.05% Tween 20–PBS. Toxin bound to GD1b was then revealed by addition of 100  $\mu\text{L}$  of Ultra TMB solution (Pierce) for 15 min followed by 100  $\mu\text{L}$  of 2 M H<sub>2</sub>SO<sub>4</sub> and recording of the absorbance at 450 nm on a Molecular Devices V-max ELISA microtiter plate reader (Molecular Devices Corp., Sunnyvale, CA).

Test samples consisted of 6 ng/mL CT B<sub>5</sub>–HRP conjugate preincubated with various concentrations of potential ligand for 2 h at room temperature. All experiments were carried out in triplicate for a given glycopolymer and validated against concentration gradients of 0, 3, 6, 15, 20, and 25 ng/mL CTB–HRP conjugate. IC<sub>50</sub> values were calculated from at least five different concentrations of competitive ligand via nonlinear regression, as described previously,<sup>39</sup> with the statistical package Microcal Origin.

### Fluorescence Titration Assay

The fluorescence titration assay used was a variation of the one described by Vrasidas et al.<sup>29</sup> All spectra were recorded on a FluoroMax-3 Fluorometer (JY Horiba, Edison, NJ) between 300 and 400 nm, using an irradiation wavelength of 282 nm. All spectra were recorded as the average of three scans at 50 nm/min. A typical experiment was as follows: To a cuvette (1  $\times$  1 cm<sup>2</sup>) was added a solution of 0.5  $\mu\text{M}$  CT B<sub>5</sub> (100  $\mu\text{L}$ ) dissolved in 10 mM PBS, pH 7.2, 150 mM NaCl. To this was added incremental quantities of a solution containing the glycopolymer and 0.5  $\mu\text{M}$  CT B<sub>5</sub> (500  $\mu\text{L}$ ). For all compounds, an additional spectrum of a reference cuvette with the same amount of ligand but no CT B<sub>5</sub> was taken and subtracted from those in which the CT B<sub>5</sub> was present. This was done to correct for low levels of inherent ligand fluorescence. The samples were left to incubate for 10 min after each addition before the measurement was started.

The fluorescence spectra were quantified via use of the center of spectral mass  $\langle \nu \rangle$  (COSM) according to eq 1<sup>40</sup>

$$\langle \nu \rangle = \frac{\sum (F_i \nu_i)}{\sum F_i}$$

where  $F_i$  is the fluorescence emission at wavenumber  $\nu_i$ , and the summation is carried out over the range cited above. A plot of the change in the center of spectral mass as a function of the log of the inhibitor concentration provided the desired dose–response curve. The data were

normalized to a maximum COSM shift of 10 to aid in data comparison. The effective concentration of inhibitor that resulted in 50% of the total change in the COSM ( $EC_{50}$ ) was determined via nonlinear regression analysis as described for the DELA studies. Errors are reported as the standard deviation of the average of multiple measurements (duplicate or triplicate) for a given ligand.

## Results

### Synthesis and Characterization of N-Glycopolypeptides

The glycopolypeptides were synthesized via amide bond formation between the amine functionality of the desired saccharide and the carboxylic group of PGA in the presence of HBTU as the condensation reagent. The reaction mixture was dialyzed against 1 M NaCl to remove impurities from the coupling reaction followed by dialysis with deionized water to remove salt. NMR experiments were conducted to determine the degree of substitution as well as the stereochemistry at the anomeric center. The  $^1\text{H}$  spectra of the glycopolymers were recorded in either  $\text{DMSO-}d_6$  or  $\text{D}_2\text{O}$  under standard quantitative conditions at ambient temperature. A typical NMR spectrum is shown in Figure 1; the lack of sharp resonances indicates the absence of starting materials in the isolated product and the successful coupling of the saccharide to the PGA.

The degrees of substitution (DS), listed in Table 1, are reported as the average fraction of substituted residues. The DS was estimated by integrating the peak areas of the saccharide H-2 proton (c, 1H), Gal ring protons (d, 5H), and the methylene protons from the caproyl-linker region (e, 10H) with respect to the polypeptide  $\beta$ - and  $\gamma$ -methylene protons (g/f, 4H). The average mole fraction of substituted residues was then calculated by using the manufacturer's reported degree of polymerization for the PGA (DP = 113). Glycopolymers with different degrees of substitution, ranging from approximately 10% to 100%, were obtained. A maximum DS of approximately 50% was obtained for the series of glycopolymers **1–3**, while a maximum DS of 100% was possible for the series of glycopolymers **4–6**, likely resulting from the improved nucleophilicity of the *N*-( $\epsilon$ -aminocaproyl)- $\beta$ -D-galactosylamine over the  $\beta$ -D-galactosylamine. The  $\beta$ - stereochemistry of the  $\gamma$ -carboxamide of the modified glutamic acid was confirmed from the chemical shift (4.81 ppm) and the  $J_{\text{H-H}}$  coupling constant (8.5 Hz) of the anomeric proton, in agreement with previously reported results for N- $\beta$ -linked poly(L-glutamic acid)-modified neoglycoconjugates.<sup>35–38</sup> These results were reproducibly obtained from multiple syntheses of glycopolymers with the targeted degrees of substitution listed in Table 1.

Select functionalized polymers were also characterized via gel permeation chromatography (GPC, Waters Corp., Milford, MA) and anionic exchange chromatography (AEC, GE Healthcare, Piscataway, NJ) to further confirm saccharide attachment. GPC results confirmed that the glycopolymers had a larger molecular weight relative to the unfunctionalized PGA (data not shown). AEC results showed a reduced overall net negative charge for the glycosylated PGA relative to the unfunctionalized PGA, also indicating successful coupling between PGA and the pendant saccharide. The random coil character of even the fully glycosylated polypeptide glycopolymer **6** in the binding assay buffer at room temperature was confirmed via circular dichroism measurements (data not shown).

### CT GD1b Direct Enzyme-Linked Assay

The potential of these glycopolypeptides to inhibit the cholera toxin was tested using a direct-enzyme linked assay (DELA) developed by Minke et al.<sup>25</sup> Inhibition curves from the DELA experiment for glycopolymers **1–6**, galactose, and the PGA backbone are shown in Figure 2.

The concentrations of samples of glycopolymers **1–6** ranged from 0  $\mu\text{M}$  to 8 mM (saccharide concentration), PGA from 0  $\mu\text{M}$  to 1 mM (protein concentration), and galactose from 0  $\mu\text{M}$  to 500 mM. As is indicated in Figure 2, compounds **1–6** showed increased inhibitory activity relative to the monovalent galactose, whereas the PGA backbone was shown to have no significant inhibitory activity below a protein concentration of 1 mM. More specifically, nonlinear regression analysis provided  $\text{IC}_{50}$  values (see Table 2) of approximately 158, 214, and 14 000  $\mu\text{M}$  for glycopolymers **1–3** and 58, 50, and 2100  $\mu\text{M}$  for glycopolymers **4–6**. Monovalent galactose exhibited an  $\text{IC}_{50}$  of 32 mM in these assays, which is consistent with previously reported values.<sup>25</sup> Also, it should be noted that the reported  $\text{IC}_{50}$  values were consistent between multiple batches of glycopolymers with similar degrees of substitution.

### Fluorescence Titration Assay

The inhibitory activity of the glycopolymers was also determined via fluorescence spectroscopy according to Vrasidas et al.,<sup>29</sup> for comparison to the DELA assays. The concentrations of glycopolymers **1** and **3** used in these experiments ranged from 0 to 3000  $\mu\text{M}$  (saccharide concentration), **4–6** from 0 to 5000  $\mu\text{M}$  (saccharide concentration), galactose from 0 to 220 mM, and the PGA backbone from 0 to 2600  $\mu\text{M}$  (protein concentration). The fluorescence spectrum for the titration with galactose is shown in Figure 3a. As is shown in the figure, an increase in inhibitor concentration results in a blue shift in the emission spectrum, in addition to a decrease in the fluorescence intensity, as has also been observed for other ligands of CT.<sup>41</sup> A similar trend was seen for all glycopolymers (representative data shown in Figure 3b). The difference in the center of spectral mass, relative to the peak maximum for the CT B<sub>5</sub> without any added inhibitor, was plotted as a function of the log of inhibitor concentration as shown in Figure 3c. The data were fit to a dose–response curve as described for the DELA, which provided the desired  $\text{EC}_{50}$  values shown in Table 2. Inspection of Figure 3c clearly shows that all glycopolymers tested bind more efficiently to CT than galactose, consistent with the DELA results. As shown in Table 2, glycopolymers **1**, **3**, and **4–6** had  $\text{EC}_{50}$  values of 354, > 3000, 77, 42, and 520  $\mu\text{M}$ , respectively, compared to 23 mM for galactose. The PGA backbone was shown to have no effect on the fluorescence to concentrations of 177  $\mu\text{M}$  (with respect to the PGA backbone), which is twice the maximum concentration of PGA (on a protein concentration basis) employed in the assays for the glycopolymers.

## Discussion

### Effect of Saccharide Density on Toxin Inhibition

With ultimate goals toward the design of protein-based glycopolymers, one of the goals of this work was to determine the effects, on toxin inhibition, of altering the saccharide density along the polymer backbone. Two different sets of glycopolypeptides, in which the number of saccharides along the backbone was varied, were produced in order to probe this effect. The first set (**1–3**) was modified with  $\beta$ -D-galactosylamine, while the second set (**4–6**) was modified with *N*-( $\epsilon$ -aminocaproyl)- $\beta$ -D-galactosylamine. The ability of these glycopolymers to inhibit the adhesion of CT B<sub>5</sub> to GD1b was tested via DELA and fluorescence spectroscopy. A closer examination of the  $\text{IC}_{50}$  values obtained from the DELA experiments, as illustrated in Figure 4a and b, indicates that an increase in saccharide density is accompanied by a decrease in toxin inhibition (or an increase in the  $\text{IC}_{50}$ ) for both sets of glycopolymers. Specifically, glycopolymer **1** had a DS of ~12% and an  $\text{IC}_{50}$  of 158  $\mu\text{M}$ , whereas **3** had a DS of ~50% and an  $\text{IC}_{50}$  of over 14 mM; similarly, the DS for **4** was ~11% with an  $\text{IC}_{50}$  of 58  $\mu\text{M}$  compared to **6** with a DS of ~100% and an  $\text{IC}_{50}$  of over 2 mM.

Improvements in inhibition as a result of potential electrostatic interactions between the negatively charged PGA backbone (at low saccharide densities) and the CT B<sub>5</sub> are not indicated

to play a role in the inhibition of CT by these glycopolypeptides, as unmodified PGA showed no sign of inhibition (Figure 2 and Figure 3c). Therefore, improvement in inhibition with decreasing saccharide density likely reflects improvements in the accessibility of the saccharide moieties in the binding event. Although the exact positions of the saccharide moieties on these PGA-based glycopolymers cannot be determined, a qualitative estimate of saccharide spacing may be deduced if the pendant carbohydrate moieties are assumed to be evenly spaced along the PGA backbone, and if the PGA backbone is approximated, under the most flexible and least flexible conditions, as a freely jointed and an extended chain, respectively. Applying the freely jointed chain<sup>42</sup> (Supporting Information) and the extended chain<sup>43</sup> (Supporting Information) as limiting cases provides approximate average distances between adjacent saccharides between 12 and 36 Å for **1** and **4**, between 8 and 18 Å for **2** and **5**, between 5 and 7 Å for **3**, and approximately 4 Å for **6**.

That inhibition is increased as the approximate distance between saccharide units is increased likely reflects the fact that adjacent binding sites on the B<sub>5</sub> subunit are separated by a distance of approximately 35 Å.<sup>33</sup> At low saccharide densities, therefore, it is plausible that the saccharides are presented at distances more consistent with the receptor spacing of CT B<sub>5</sub> and bind more efficiently on a per-saccharide basis. This phenomenon results in a decrease in the IC<sub>50</sub> value, relative to the more densely functionalized glycopolymers in which the saccharides are less effectively utilized in binding. Indeed, results relating minimum distances required for optimal (maximum) binding of linear molecules to CT have been reported in the study of bivalent inhibitors of CT<sup>33</sup> and SLT.<sup>22</sup> The small or negligible differences in inhibition values observed for **1** versus **2** and **4** versus **5**, respectively, may reflect their compositional heterogeneity, which results in similarities between the saccharide densities of the relevant glycopolypeptides but is unavoidable upon chemical modification of the already polydisperse PGA. Nevertheless, the results demonstrate the increasing IC<sub>50</sub> values with increasing saccharide density. That the more densely functionalized glycopolymers exhibit higher IC<sub>50</sub> values likely also reflects steric interference of saccharide binding by other nearby saccharides. A similar interpretation has been previously suggested, on the basis of molecular modeling investigations, for the reduction in inhibition of erythrocyte agglutinating activity by 7-oxanorbornene-based neoglycopolymers containing glucose or mannose of increasing densities.<sup>44</sup> Additionally, in studies of the clustering of Con A by similar neoglycopolymers of varying mannose density, glycopolymers with a relatively low binding epitope density exhibited the most efficient binding on a binding epitope basis.<sup>45</sup>

### Effect of Saccharide Linker Arm Length on Toxin Inhibition

An additional goal of this work was to determine the effect of the saccharide linker arm length on the inhibition of CT B<sub>5</sub> by the poly(L-glutamic acid)-based glycopolymers. As mentioned above, two sets of glycopolymers, derivatized with either β-D-galactosylamine or N-(ε-aminocaproyl)-β-D-galactosylamine, were synthesized for these studies. As illustrated in Table 2 and Figure 4, glycopolymers **4–6** exhibited greater inhibitory power than **1–3** at all saccharide densities. A comparison of the two most effective inhibitors (**1** and **4**) revealed that **4** (IC<sub>50</sub> of 58 μM) was approximately three times as effective as **1** (IC<sub>50</sub> of 158 μM) at preventing bacterial adhesion of the cholera toxin B<sub>5</sub> subunit in the DELA experiments. A similar trend was seen in the fluorescence assay in which **4** (EC<sub>50</sub> of 77 μM) was approximately 5 times more effective as **1** (EC<sub>50</sub> of 354 μM).

Analysis of the interaction between the B<sub>5</sub> subunit and the natural CT B<sub>5</sub> ligand GM1 reveals that the oligosaccharide resides in a cleft approximately 16 Å deep (Supporting Information).

---

**Supporting Information Available.** Calculation of the approximate distances between adjacent carbohydrate moieties along the PGA backbone. Estimation of the depth of the CT B<sub>5</sub> binding pocket and linker arm length of the pendent saccharides. This information is available free of charge via the Internet at <http://pubs.acs.org>.



Estimations of the length of the respective linker arms in an extended chain conformation (Supporting Information) yields approximate distances, between the  $\alpha$ -carbon on the poly(L-glutamic acid) backbone and the C4 carbon of the pendant galactose, of 9.6 Å and 18.7 Å for glycopolymers **1–3** and **4–6**, respectively. These results strongly suggest that the increased inhibition by glycopolymers **4–6** results from improvements in the accessibility of the terminal galactopyranoside provided by the 6-aminohexanoic acid linker arm. Similar improvements in inhibition by the monovalent *N*-( $\epsilon$ -amino-caproyl)- $\beta$ -D-galactosylamine versus D-galactose (35-fold improvement)<sup>25</sup> also suggests that hydrophobic interactions between the aliphatic region of the linker arm with residues Tyr12 and Trp88, located in the binding pocket, may provide favorable interactions apart from improved accessibility.<sup>29</sup> This supposition is further supported by reports of CT inhibition by a series of 3,5-substituted phenyl galactosides.<sup>46</sup> In particular, functionalization of *m*-nitrophenyl- $\alpha$ -D-galactopyranoside (MNPG) with 1,4-bis(3-aminopropyl)piperazine (APP-MNPG) yielded a MNPG derivative (IC<sub>50</sub> of 200  $\mu$ M) with a sixfold improvement over MNPG (IC<sub>50</sub> of 1.4 mM). The gain in avidity was attributed to the hydrophobic interactions of the propylpiperazine with residues in the binding pocket.

### Possible Mechanism of Inhibition

Multivalent ligands can cause improvements in binding over monovalent ligands via many possible mechanisms including aggregation, subsite binding, receptor clustering, chelate effects, and/or steric stabilization.<sup>18</sup> As no aggregation was observed during the assays and as the receptor sites on the surface of the CT B<sub>5</sub> subunit are well-defined and unable to cluster, the contributions from aggregation, subsite binding, and receptor clustering are likely to be negligible. The observed inhibition of CT B<sub>5</sub> by glycopolymers **1–6** in the DELA assays therefore likely results from the chelate effect and/or steric stabilization, which would prevent interaction of the toxin with the GDIb. Steric stabilization effects have been invoked previously for the inhibition of CT by bivalent inhibitors<sup>33</sup> and the inhibition of the influenza virus via linear glycopolymers.<sup>5</sup> One possible approach to distinguish between the two mechanisms would be to demonstrate a significant degree of binding between the inhibitor and the toxin in solution, thus ruling out steric stabilization as a major mode of inhibition.

In these investigations, a fluorescence titration assay was used to monitor the binding of inhibitor to CT B<sub>5</sub> in solution, via the shift in the center of spectral mass of the characteristic fluorescence emission from the single Trp residue in each of the five subunits. The shift in the COSM ranged from 6 to 16 nm for glycopolymers **1–6** upon association with the B<sub>5</sub> subunit (see Figure 3), in agreement with the previously reported 12 nm bathochromic shift in the Trp88 emission spectra upon CT B<sub>5</sub> association with GM1.<sup>41</sup> In addition, the EC<sub>50</sub> values obtained from fluorescence measurements for **1–6** are in excellent agreement with the IC<sub>50</sub> values determined via the DELA (Table 2). If steric stabilization were the primary mode of inhibition, IC<sub>50</sub> values obtained via DELA experiments would be expected to be lower than those obtained from the solution-phase fluorescence assay. The agreement of the results from the two assays therefore suggests that improvements in glycopolymer binding versus the monovalent saccharide reflect increased binding avidity under equilibrium conditions via a chelate effect, in contrast to the steric mechanisms proposed for bivalent inhibitors. These results may also suggest a potentially greater impact of variations in glycopolymer architecture on inhibition of CT by these types of linear glycopolymers, as the inhibition appears to occur via solution-phase binding rather than as a result of aggregation or steric stabilization. Such effects need to be verified on a glycopolymer-to-glycopolymer basis to determine if this trend holds for an expanded set of linear polypeptide-based glycopolymers.

## Conclusions

A series of glycopolymers with a polyglutamic acid-based backbone have been produced with variations in the density and linker length of the pendant carbohydrate moiety. Results obtained from competitive enzyme-linked immunosorbent assays and fluorescence titration experiments suggest an optimal saccharide density for CT inhibition by the linear glycopolymers. A decrease in the approximate distances between adjacent saccharide units was accompanied with a decrease in the inhibitory activity of compounds 1–6. Second, increasing the length and hydrophobicity of the linker arm has been shown to improve inhibition in these linear glycopolymers, as has been previously suggested in investigations of small-molecule and dendrimeric inhibitors. Finally, the similarities between DELA and fluorescence titration results suggest that these glycopolymers inhibit CT via a competitive mechanism rather than steric stabilization. Synthesis of future linear inhibitors, in which the spacing of saccharides with hydrophobic linker arms can be well-controlled and tailored to better match those of the B<sub>5</sub> subunit, may therefore yield materials with enhanced inhibitory activity. Accordingly, the results from this work are being applied toward the design of well-defined, linear glycopolypeptides, produced via protein engineering methods, for the inhibition of bacterial toxins and other lectin targets.

## Acknowledgment

This work was supported by grants from the National Institutes of Health (1-P20-RR17716-01), the U.S. Army Research Office, and the University of Delaware Research Foundation. We thank Dr. Steven Bai (University of Delaware) for assistance with NMR spectroscopy and Mr. John Dykins (University of Delaware) with helpful discussion and assistance with various mass spectroscopies.

## References and Notes

1. Varki A. *Glycobiology* 1993;3(2):97–130. [PubMed: 8490246]
2. Ambrosi M, Cameron NR, Davis BG, Stolnik S. *Org. Biomol. Chem* 2005;3(8):1476–1480. [PubMed: 15827644]
3. Lis H, Sharon N. *Chem. Rev* 1998;98(2):637–674. [PubMed: 11848911]
4. Dimick SM, Powell SC, McMahon SA, Moothoo DN, Naismith JH, Toone EJ. *J. Am. Chem. Soc* 1999;121(44):10286–10296.
5. Mammen M, Chio S-K, Whitesides GM. *Angew. Chem., Int. Ed* 1998;37(20):2755–2794.
6. Baird EJ, Holowka D, Coates GW, Baird B. *Biochemistry* 2003;42:12739–12748. [PubMed: 14596588]
7. Dam TK, Oscarson S, Roy R, Das SK, Page D, Macaluso F, Brewer CF. *J. Biol. Chem* 2005;280:8640–8646. [PubMed: 15632152]
8. Gordon EJ, Sanders WJ, Kiessling LL. *Nature (London)* 1998;392:30–31. [PubMed: 9510244]
9. Reuter JD, Myc A, Hayes MM, Gan Z, Roy R, Yin R, Piehler LT, Esfand R, Tomalia DA, Baker JRJ. *Bioconjugate Chem* 1999;10:271–278.
10. Roy R. *Trends Glycosci. Glycotechnol* 2003;15:291–310.
11. Woller EK, Walter ED, Morgan JR, Singel DJ, Cloninger MJ. *J. Am. Chem. Soc* 2003;125:8820–8826. [PubMed: 12862477]
12. Gordon EJ, Strong LE, Kiessling LL. *Bioorg. Med. Chem* 1998;6(8):1293–1299. [PubMed: 9784870]
13. Nagahori N, Nishimura S-I. *Biomacromolecules* 2001;2(1):22–24. [PubMed: 11749149]
14. Mammen M, Dahmann G, Whitesides GM. *J. Med. Chem* 1995;38(21):4179–4190. [PubMed: 7473545]
15. Kamitakahara H, Suzuki T, Nishigori N, Suzuki Y, Kanie O, Wong C-H. *Angew. Chem., Int. Ed* 1998;37(11):1524–1528.
16. Mangold SL, Morgan JR, Strohmeyer GC, M GA, Cloninger MJ. *Org. Biomol. Chem* 2005;3(12):2354–2358. [PubMed: 16010372]

17. Woller EK, Cloninger MJ. *Org. Lett* 2002;4(1):7–10. [PubMed: 11772077]
18. Gestwicki JE, Cairo CW, Strong LE, Oetjen KA, Kiessling LL. *J. Am. Chem. Soc* 2002;124(50):14922–14933. [PubMed: 12475334]
19. Fan E, Merritt EA, Verlinde CLMJ, Hol WGJ. *Curr. Opin. Struct. Biol* 2000;10(6):680–686. [PubMed: 11114505]
20. Gargano JM, Ngo T, Kim JY, Acheson DW, Lees WJ. *J. Am. Chem. Soc* 2001;123(51):12909–12910. [PubMed: 11749553]
21. Kitov PI, Sadowska JM, Mulvey G, Armstrong GD, Ling H, Pannu NS, Read RJ, Bundle DR. *Nature (London)* 2000;403(6770):669–672. [PubMed: 10688205]
22. Kitov PI, Shimizu H, Homans SW, Bundle DR. *J. Am. Chem. Soc* 2003;125(11):3284–3294. [PubMed: 12630884]
23. Liu J, Zhang Z, Tan X, Hol WGJ, Verlinde CLMJ, Fan E. *J. Am. Chem. Soc* 2005;127(7):2044–2045. [PubMed: 15713072]
24. Minke WE, Hong F, Verlinde CLMJ, Hol WGJ, Fan E. *J. Biol. Chem* 1999;274(47):33469–33473. [PubMed: 10559230]
25. Minke WE, Roach C, Hol WGJ, Verlinde CLMJ. *Biochemistry* 1999;38(18):5684–5692. [PubMed: 10231518]
26. Thobhani S, Ember B, Siriwardena A, Boons G-J. *J. Am. Chem. Soc* 2003;125:7154–7155. [PubMed: 12797770]
27. Thompson JP, Schengrund C-L. *Glycoconjugate J* 1997;14(7):837–845.
28. Thompson JP, Schengrund C-L. *Biochem. Pharmacol* 1998;56(5):591–597. [PubMed: 9783728]
29. Vrasidas I, De Mol NJ, Liskamp RMJ, Pieters RJ. *Eur. J. Org. Chem* 2001;24:4685–4692.
30. Zhang Z, Liu J, Verlinde CLMJ, Hol WGJ, Fan E. *J. Org. Chem* 2004;69(22):7737–7740. [PubMed: 15498005]
31. Spangler BD. *Microbiol. Rev* 1992;56:622–647. [PubMed: 1480112]
32. Fan E, Zhang Z, Minke WE, Hou Z, Verlinde CLMJ, Hol WGJ. *J. Am. Chem. Soc* 2000;122(11):2663–2664.
33. Pickens JC, Mitchell DD, Liu J, Tan X, Zhang Z, Verlinde CLMJ, Hol WGJ, Fan E. *Chem. Biol* 2004;11(9):1205–1215. [PubMed: 15380181]
34. Lundquist JJ, Debenham SD, Toone EJ. *J. Org. Chem* 2000;65(24):8245–8250. [PubMed: 11101380]
35. Zeng X, Murata T, Kawagishi H, Usui T, Kobayashi K. *Biosci. Biotechnol. Biochem* 1998;62(6):1171–1178. [PubMed: 9692202]
36. Zeng X, Murata T, Kawagishi H, Usui T, Kobayashi K. *Carbohydr. Res* 1998;312(4):209–217. [PubMed: 9861697]
37. Zeng X, Nakaaki Y, Murata T, Usui T. *Arch. Biochem. Biophys* 2000;383(1):28–37. [PubMed: 11097173]
38. Totani K, Kubota T, Kuroda T, Murata T, Hidari KIPJ, Suzuki T, Suzuki Y, Kobayashi K, Ashida H, Yamamoto K, Usui T. *Glycobiology* 2003;13(5):315–326. [PubMed: 12626382]
39. Bowen WP, Jerman JC. *Trends Pharmacol. Sci* 1995;16(12):413–417. [PubMed: 8578614]
40. Lima LMTR, Zingali RB, Foguel D, Monteiro RQ. *Eur. J. Biochem* 2004;271(17):3580–3587. [PubMed: 15317594]
41. Mertz JA, McCann JA, Picking WD. *Biochem. Biophys. Res. Commun* 1996;226(1):140–144. [PubMed: 8806604]
42. Sperling, LH. *Introduction to Physical Polymer Science*. Vol. 3rd ed.. New York: John Wiley & Sons, Inc.; 2001.
43. Creighton, TE. *Proteins: Structures and Molecular Properties*. New York: W. H. Freeman Company; 1992.
44. Schuster MC, Mortell KH, Hegeman AD, Kiessling LL. *J. Mol. Catal* 1997;116(1–2):209–216.
45. Cairo CW, Gestwicki JE, Kanai M, Kiessling LL. *J. Am. Chem. Soc* 2002;124(8):1615–1619. [PubMed: 11853434]
46. Mitchell DD, Pickens JC, Korotkov K, Fan E, Hol WGJ. *Bioorg. Med. Chem* 2004;12(5):907–920. [PubMed: 14980603]

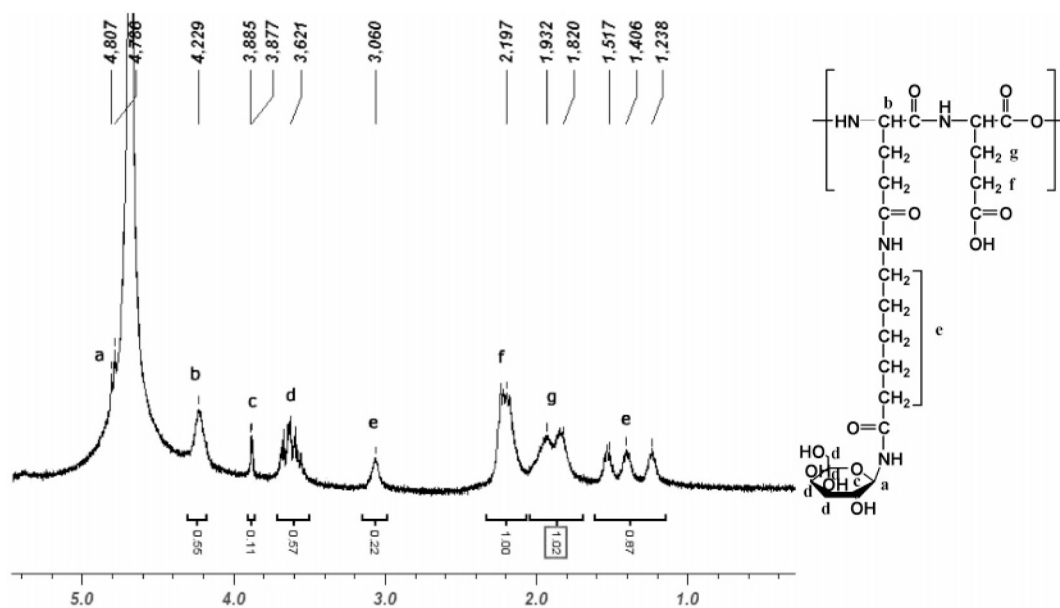


**Figure 1.**  
 $^1\text{H}$  NMR spectrum of glycopolymer **5** ( $\text{D}_2\text{O}$ ,  $25^\circ\text{C}$ ,  $400\text{ MHz}$ ).

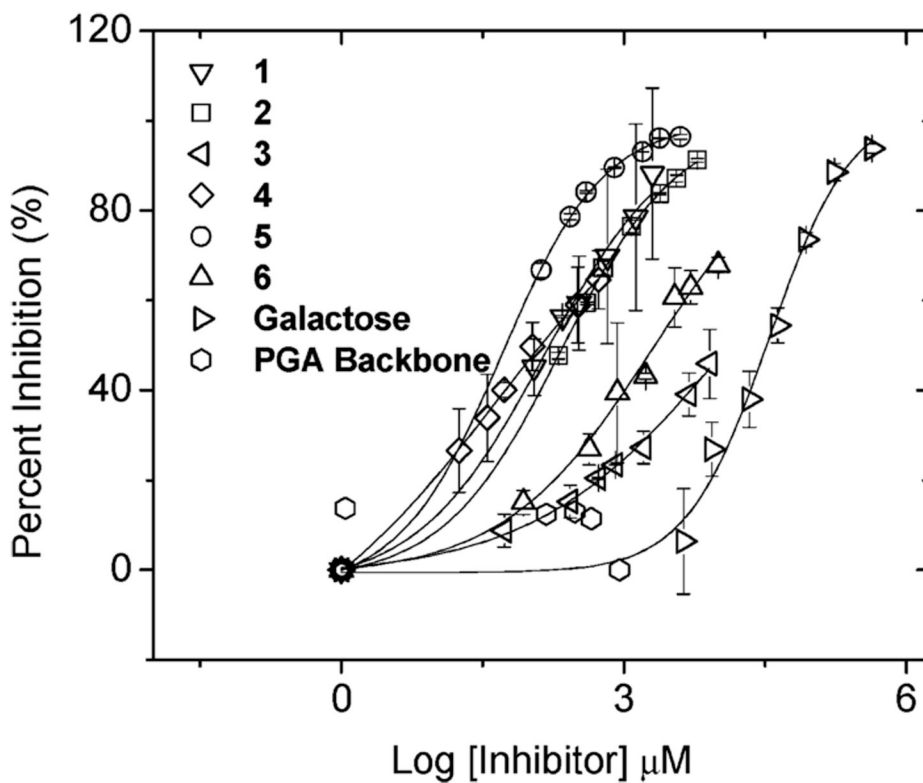


**Figure 2.** Inhibition of CT B<sub>5</sub> binding by glycopolymers **1–6** as determined via direct-linked enzyme assay. The solid line represents the best curve fit obtained by fitting the data to a dose–response curve via nonlinear regression analysis. No curve was fit to the PGA data, as it showed no inhibition. All experiments were run in triplicate; the error bars represent the standard deviation among the three trials.

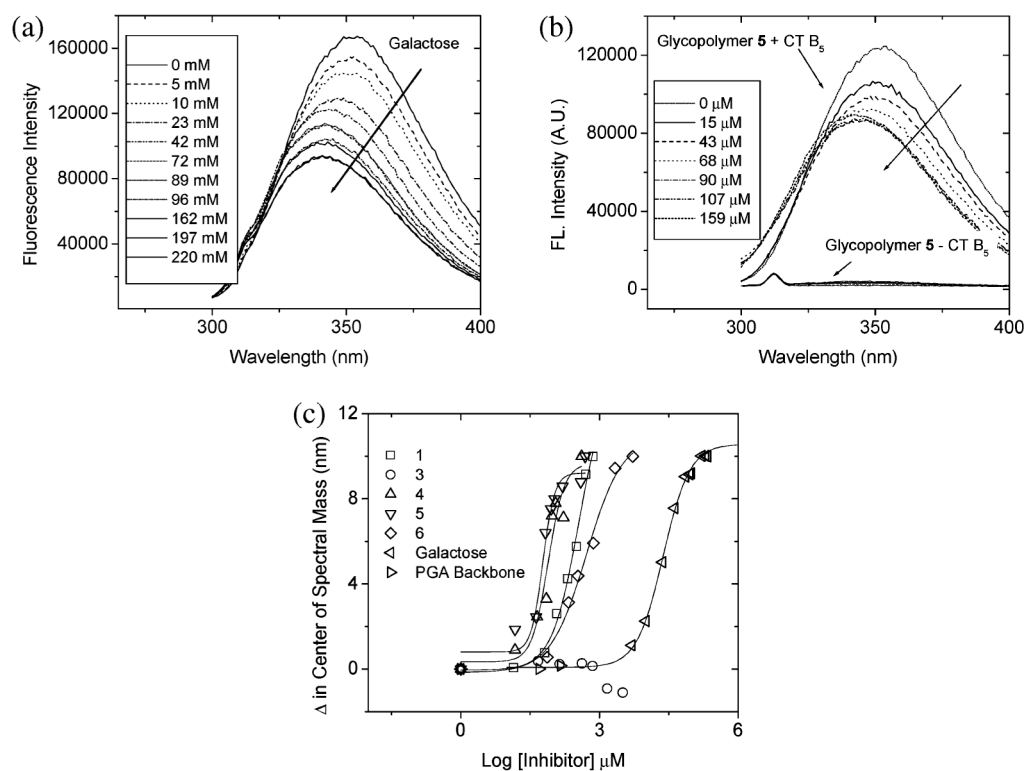


**Figure 3.** Fluorescence titration results for (a) galactose and (b) glycopolymer **5**. The arrow indicates the direction of increasing inhibitor concentration. (c) EC<sub>50</sub> plots for glycopolymers, PGA, and galactose. Increasing the inhibitor concentration results in a blue shift in fluorescence emission as well as a decrease in fluorescence intensity. Glycopolymer **3** exhibited no inhibition at all at concentrations up to 3 mM; IC<sub>50</sub> values for this compound are therefore simply specified as >3 mM.

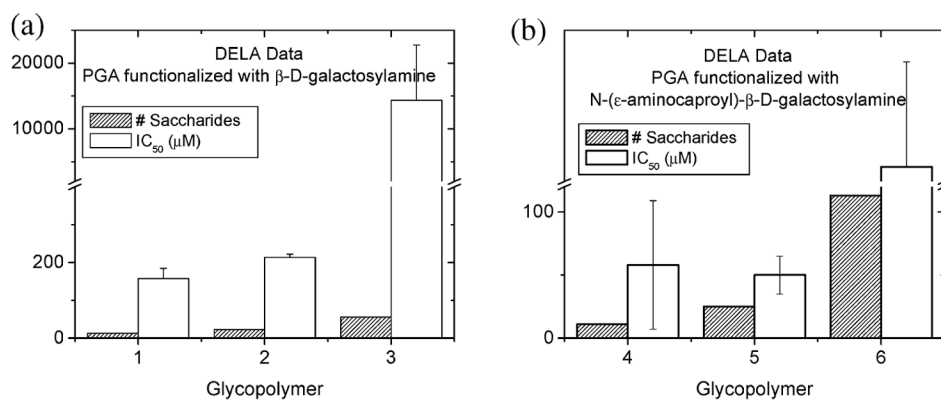


**Figure 4.** Plot of  $IC_{50}$  values as a function of increasing saccharide density: (a) glycopolymers 1–3, (b) glycopolymers 4–6. Note that the y-axis in this figure represents the average total number of saccharides on the glycopolymer, rather than the percent substitution. The data in this figure were obtained from the DELA experiments.

**Table 1**Compositions of Synthesized Glycopolymers<sup>a</sup>

Sample	DS (mol %)	Type of Saccharide
Galactose	N/A	Galactose
<b>1</b>	12.0 ± 1.6	β-D-galactosylamine
<b>2</b>	20.6 ± 4.3	β-D-galactosylamine
<b>3</b>	52.7 ± 5.2	β-D-galactosylamine
<b>4</b>	11.1 ± 2.2	<i>N</i> -(ε-aminocaproyl)-β-D-galactosylamine
<b>5</b>	21.3 ± 3.0	<i>N</i> -(ε-aminocaproyl)-β-D-galactosylamine
<b>6</b>	100 ± 24.3	<i>N</i> -(ε-aminocaproyl)-β-D-galactosylamine
PGA	N/A	none

<sup>a</sup>The error associated with the DS was estimated via the integration of multiple peaks in the spectrum, as delineated in the text.



**Table 2**DELA and Fluorescence Titration Results for Glycopolymer-Cholera Toxin Binding Assays<sup>a</sup>

Sample	IC <sub>50</sub> (DELA) (mM)	EC <sub>50</sub> (fluorescence) (mM)
galactose	32 ± 6.20	23 ± 7.1
<b>1</b>	0.158 ± 0.027	0.354 ± 0.11
<b>2</b>	0.214 ± 0.008	N.D.
<b>3</b>	14.0 ± 8.40	>3.00
<b>4</b>	0.058 ± 0.051	0.077 ± 0.024
<b>5</b>	0.050 ± 0.015	0.042 ± 0.025
<b>6</b>	2.1 ± 0.840	0.520 ± 0.16
PGA	none	none

<sup>a</sup> Errors are reported as the standard deviations of the average value obtained from multiple assays of a given inhibitor.